Chapter 3

Saltwater Intrusion in the Changjiang Estuary

Jianrong Zhu, Hui Wu, Lu Li and Cheng Qiu

Additional information is available at the end of the chapter

http://dx.doi.org/10.5772/intechopen.80903

Abstract

Saltwater intrusion in the Changjiang Estuary and the impacts of river discharge, tide, wind, sea level rise, river basin, and major estuary projects on saltwater intrusion are studied in this chapter. There is a net landward flow in the NB (North Branch) when river discharge is low during spring tide, resulting in a type of saltwater intrusion known as the SSO (saltwater-spilling-over from the NB into the SB (South Branch)), which is the most striking characteristic of saltwater intrusion in the estuary. A three-dimension numerical model with HSIMT-TVD advection scheme was developed to study the hydrodynamic processes and saltwater intrusion in the Changjiang Estuary. Saltwater intrusion in the estuary is controlled mainly by river discharge and tide, but is also influenced by wind, sea level rise, river basin, and estuary projects. Saltwater intrusion is enhanced when river discharge decreases. There is more time for the reservoir to take freshwater from the river when river discharge is larger. The fortnightly spring tide generates greater saltwater intrusion than the neap tide. The saltwater intrusion in the SP (South Passage) is stronger than that in the NP (North Passage), and the intrusion in the NP is stronger than that in the NC (North Channel). The northerly wind produces southward currents along the Subei coast as well as the landward Ekman transport, which enhances the saltwater intrusion in the NC and NB and weakens the saltwater intrusion in the NP and SP. Saltwater intrusion becomes stronger as the sea level rises and is much stronger when river discharge is much small. The DWP (Deep Waterway Project) alleviates the saltwater intrusion in the NC and the lower reaches of the NP and enhances the saltwater intrusion in the SP and in the upper reaches of the NP. The Three Gorges Dam (TGD) increases river discharge in winter, which weakens saltwater intrusion, and is favorable for reducing the burden of freshwater supplement in the highly populated estuarine region. The Water Diversion South to the North Project (WDP) decreases river discharge, enhances saltwater intrusion, and is unfavorable for freshwater supply in the estuary.

Keywords: Changjiang Estuary, saltwater intrusion, dynamic process, numerical model, freshwater resource

1. Introduction

The Changjiang, also known as the Yangtze River, is one of the largest rivers in the world. The Changjiang Estuary has a 90-km-wide river mouth, which is characterized by multiple bifurcations (**Figure 1**). First, the estuary is divided by Chongming Island into the South Branch (SB) and North Branch (NB). The SB and its lower reaches form the main channel of the Changjiang and discharge most of the river discharge, while the NB is heavily silted. Second, the lower SB is bifurcated into the South Channel (SC) and North Channel (NC) by Changxing Island and Hengsha Island. Finally, the SC is bifurcated into the South Passage (SP) and North Passage (NP) by Jiuduansha Island [1]. The Changjiang Estuary is unique among well-studied estuaries, has an extremely dynamic hydrological environment due to runoff, tide, wind, mixing, topography, and continental shelf current outside the river mouth, which are the main dynamic control factors on hydrodynamic processes in the estuary [2–4].

Saltwater intrusion in the Changjiang Estuary is controlled mainly by the river discharge and tide [2, 5–8], but is also influenced by wind [4], topography [9], river watershed and estuary projects [10–12], and sea level rise [13]. The natural evolution and artificial reclamation of the intertidal zone from the 1950s to the 2000s have severely narrowed the upper reaches of the NB [14]. As a consequence, the upper reaches of the NB have become almost orthogonal to the SB, while the lower reaches have become funnel shaped. The evolution of river regime of the NB helps to prevent runoff from entering the NB, especially during the dry season; meanwhile, it makes the tidal range larger in the NB than in the SB. Strong tidal forcing in the NB induces significant subtidal circulation, resulting in a net landward flow when river discharge is low during spring tide [1]. This residual transport forms a type of saltwater intrusion known as the saltwater-spilling-over (SSO) from the NB into the SB, which is the most striking characteristic of saltwater intrusion in the estuary. During spring tide, the water level rises considerably in the upper reaches of the NB due to its funnel shape, leading to a massive amount of saline water spilling over the shoals into the SB [1]. The saline water that spilled into the SB is then transported downstream forced by runoff and arrives in the middle reaches of the SB during

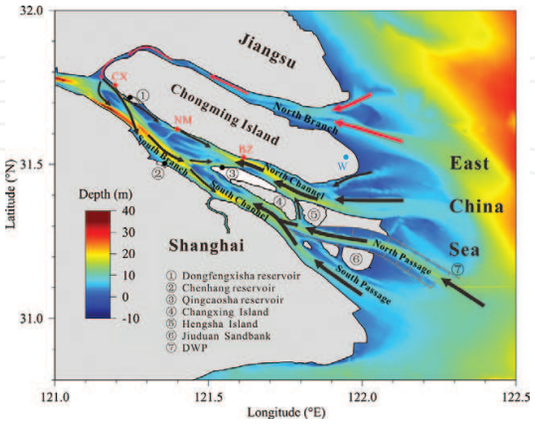

Figure 1. Map of the Changjiang Estuary and the pathways of saltwater intrusion (arrows). Key geographic locations and hydrologic stations are marked. The red dots indicate the locations of Baozhen (BZ) and Chongxi (CX) hydrologic stations. The black dots indicate the locations of water intakes of the reservoirs. W is the location of the weather station at the Chongming eastern shoal. DWP stands for the deep waterway project.

the subsequent neap tide. This process impacts the water intakes of the Dongfengxisha, Chenhang, and Qingcaosha reservoirs and threatens the freshwater supply to Shanghai, a megacity in China.

The Changjiang Estuary has been the most important freshwater resource for Shanghai. The huge QCSR (Qingcaosha reservoir) was built in 2010 along northwestern Changxing Island, supplying more than 70% of the freshwater for the 13 million people in Shanghai. The QCSR takes the water from the Changjiang when the salinity is lower than 0.45 (the salinity standard of drinking water), but it suspends its operation when the saltwater intrusion influences the water intake. In order to understand the dynamic processes and mechanism of saltwater intrusion in the Changjiang Estuary, we studied the impacts of tide, river discharge, wind, sea level rise, river basin, and major estuary projects on saltwater intrusion, which not only has important scientific significance, but also has great application meaning for safety of freshwater resource in Shanghai.

Estuarine saltwater intrusion is a common phenomenon, which can produce estuarine circulation [15] and change stratification [16], thereby influencing sediment transport, producing peak estuarine turbidity [17], and degrading the safety of freshwater intake of estuarine reservoirs.

In this chapter, we analyze and simulate the saltwater intrusion in the Changjiang Estuary. In Section 2, we describe the numerical model used to simulate the saltwater intrusion in the estuary. In Section 3, we first simulate the saltwater intrusion in a climatological state under various dynamic factors, and then analyze the impacts of river discharge, tide, wind, sea level rise, river watershed, and artificial estuary projects on the saltwater intrusion by numerical experiments. In Section 4, a summary is provided.

2. Numerical model

ECOM-si was developed based on the Princeton Ocean Model (POM; [18, 19]) with several improvements [20] to address the demand for numerical simulations of water body bounded by complicated coastlines. This model incorporates the Mellor-Yamada level-2.5 turbulent closure scheme to provide a time and space dependent parameterization of vertical turbulent mixing [21–23]. This model was further developed by Wu and Zhu [24] using the third HSIMT-TVD scheme for the advection term in the mass transport equation. This scheme is flux-based, with third order accuracy in space, second order accuracy in time, and no numerical oscillation.

Under the assumption of incompressibility, Boussinesq and hydrostatic approximations, and using the horizontal nonorthogonal curvilinear and vertical stretched sigma coordinate system, the governing equations of ocean circulation and water mass (consisting of momentum, continuity, temperature, salinity, and density equations) are as follows [25]:

$$\begin{aligned}&\frac{\partial DJu_1}{\partial t}+\frac{\partial DJ\hat{U}u_1}{\partial \xi}+\frac{\partial DJ\hat{V}u_1}{\partial \eta}+\frac{\partial J\omega u_1}{\partial \sigma}-Dh_2\hat{V}\left[v_1\frac{\partial}{\partial \xi}\left(\frac{J}{h_1}\right)-u_1\frac{\partial}{\partial \eta}\left(\frac{J}{h_2}\right)+Jf\right]-Dh_2u_1v_1\frac{\partial}{\partial \xi}\left(\frac{h_3}{h_1h_2}\right)\\&\quad=-h_2gD\frac{\partial \zeta}{\partial \xi}+\frac{gh_2D}{\rho_o}\frac{\partial D}{\partial \xi}\int_\sigma^0\sigma\frac{\partial \rho}{\partial \sigma}d\sigma-\frac{gh_2D^2}{\rho_o}\frac{\partial}{\partial \xi}\int_\sigma^0\rho d\sigma+\frac{1}{D}\frac{\partial}{\partial \sigma}\left(K_m\frac{\partial Ju_1}{\partial \sigma}\right)+DJF_x,\end{aligned}\tag{1}$$

$$\frac{\partial DJv_1}{\partial t}+\frac{\partial DJ\hat{U}v_1}{\partial \xi}+\frac{\partial DJ\hat{V}v_1}{\partial \eta}+\frac{\partial J\omega v_1}{\partial \sigma}+Dh_1\hat{U}\left[v_1\frac{\partial}{\partial \xi}\left(\frac{J}{h_1}\right)-u_1\frac{\partial}{\partial \eta}\left(\frac{J}{h_2}\right)+Jf\right]-Dh_1u_1v_1\frac{\partial}{\partial \eta}\left(\frac{h_3}{h_1h_2}\right)$$
$$=-h_1gD\frac{\partial \zeta}{\partial \eta}+\frac{gh_1D}{\rho_o}\frac{\partial D}{\partial \eta}\int_{\sigma}^{0}\sigma\frac{\partial \rho}{\partial \sigma}d\sigma-\frac{gh_1D^2}{\rho_o}\frac{\partial}{\partial \eta}\int_{\sigma}^{0}\rho d\sigma+\frac{1}{D}\frac{\partial}{\partial \sigma}\left(K_m\frac{\partial Jv_1}{\partial \sigma}\right)+DJF_{y,} \tag{2}$$

$$\frac{\partial \zeta}{\partial t}+\frac{1}{J}\left[\frac{\partial}{\partial \xi}\left(DJ\hat{U}\right)+\frac{\partial}{\partial \eta}\left(DJ\hat{V}\right)\right]+\frac{\partial \omega}{\partial \sigma}=0 \tag{3}$$

$$\frac{\partial JD\theta}{\partial t}+\frac{\partial JD\hat{U}\theta}{\partial \xi}+\frac{\partial JD\hat{V}\theta}{\partial \eta}+\frac{\partial J\omega\theta}{\partial \sigma}=\frac{1}{D}\frac{\partial}{\partial \sigma}\left(K_h\frac{\partial J\theta}{\partial \sigma}\right)+DJF_\theta \tag{4}$$

$$\frac{\partial JDs}{\partial t}+\frac{\partial JD\hat{U}s}{\partial \xi}+\frac{\partial JD\hat{V}s}{\partial \eta}+\frac{\partial J\omega s}{\partial \sigma}=\frac{1}{D}\frac{\partial}{\partial \sigma}\left(K_h\frac{\partial Js}{\partial \sigma}\right)+DJF_s \tag{5}$$

$$\rho_{total}=\rho_{total}\left(\theta,s\right) \tag{6}$$

where,

$$\omega=w-\sigma\left(\hat{U}\frac{\partial D}{\partial \xi}+\hat{V}\frac{\partial D}{\partial \eta}\right)-\left[(1+\sigma)\frac{\partial \zeta}{\partial t}+\hat{U}\frac{\partial \zeta}{\partial \xi}+\hat{V}\frac{\partial \zeta}{\partial \eta}\right] \tag{7}$$

In the above equations, the new coordinate (ξ, η, and σ) is defined as: $\xi=\xi(x,y),\ \eta=\eta(x,y),$ $\sigma=\frac{z-\zeta}{H+\zeta}$.

The vertical coordinate σ varies from −1 at z = −H to 0 at z = ζ, where, x, y and z are the east, north, and vertical axes of the Cartesian coordinate, respectively; ζ is the sea surface elevation; and H is the total water depth. The ξ and η components of velocity (defined as u_1, v_1) can be expressed in the forms of $u_1=\frac{h_2}{J}\left(x_\xi u+y_\xi v\right), v_1=\frac{h_1}{J}\left(x_\eta u+y_\eta v\right)$ [25], in which, u and v are the x and y velocity components, $\xi_x=\frac{y_\eta}{J}, \xi_y=-\frac{x_\eta}{J}, \eta_x=-\frac{y_\xi}{J}, \eta_y=\frac{x_\xi}{J}$, where J is the Jacobin function in the form of $J=x_\xi y_\eta-x_\eta y_\xi$, and the subscripts (ξ and η) indicate derivatives. The metric factors h_1 and h_2 of the coordinate transformation are defined as $h_1=\sqrt{x_\xi^2+y_\xi^2}$, $h_2=\sqrt{x_\eta^2+y_\eta^2}$, $\hat{U}=\frac{1}{J}\left(h_2u_1-\frac{h_3}{h_1}v_1\right), \hat{V}=\frac{1}{J}\left(h_1v_1-\frac{h_3}{h_2}u_1\right)$, in which, $h_3=y_\xi y_\eta+x_\xi x_\eta$, where θ is the water temperature, s is the salinity, f is the Coriolis parameter, g is the gravitational acceleration, K_m is the vertical eddy viscosity coefficient, and K_h is the thermal vertical eddy friction coefficient. F_u, F_v, F_θ, and F_s represent the two horizontal momentum terms, thermal term, and salt diffusion term, respectively. ρ and ρ_o are the perturbation and reference density, which satisfy $\rho_{\text{total}}=\rho+\rho_o$. F_u, F_v, F_θ, and F_s are calculated by using Smagorinsky's [26] formula in which horizontal diffusion is directly proportional to the product of horizontal grid sizes. K_m and K_h are calculated using the modified Mellor-Yamada level-2.5 turbulent closure scheme [20–22].

The surface and bottom boundary conditions for the momentum and heat equations are given by:

$$\frac{\rho_0 K_m}{D}\left(\frac{\partial u_1}{\partial \sigma},\frac{\partial v_1}{\partial \sigma}\right)=(\tau_{0\xi},\tau_{0\eta});\ \frac{\rho_0 K_H}{D}\left(\frac{\partial \theta}{\partial \sigma}\right)=Q_{net};\ \frac{\rho_0 K_H}{D}\left(\frac{\partial s}{\partial \sigma}\right)=s(\hat{P}-\hat{E});\omega=0, at\,\sigma=0,$$

$$\frac{\rho_0 K_m}{D}\left(\frac{\partial u_1}{\partial \theta},\frac{\partial v_1}{\partial \theta}\right)=(\tau_{b\xi},\tau_{b\eta});\ \frac{\partial \theta}{\partial \sigma}=0;\ \frac{\partial s}{\partial \sigma}=0;\ \omega=0, at\,\sigma=-1$$

where $(\tau_{o\xi}, \tau_{o\eta})$ and $(\tau_{b\xi},\tau_{b\eta})=C_d\sqrt{U^2+V^2}(U^2+V^2)$ are the ξ and η components of surface wind and bottom stresses; Q_{net} is the net surface heat flux; $\hat{P}$ is the precipitation flux; and $\hat{E}$ is the evaporation flux. The surface wind stress was calculated based on the neutral steady state drag coefficient developed by Large and Pond [27]. The drag coefficient C_d at the bottom is determined by matching a logarithmic bottom layer to the model at a height z_{ab} above the bottom, that is, $C_d=\max\left[k^2/\ln\left(\frac{z_{ab}}{z_0}\right)^2, 0.0025\right]$.

where $k = 0.4$ is the Karman's constant and z_0 is the bottom roughness parameter [25].

Eqs. (1)–(7) are solved prognostically as initial value problems of oceanic motion. The initial velocity takes the form $u_1 = v_1 = 0$, and the water elevation is also set to ζ = 0. The initial temperature and salinity are specified using observational data.

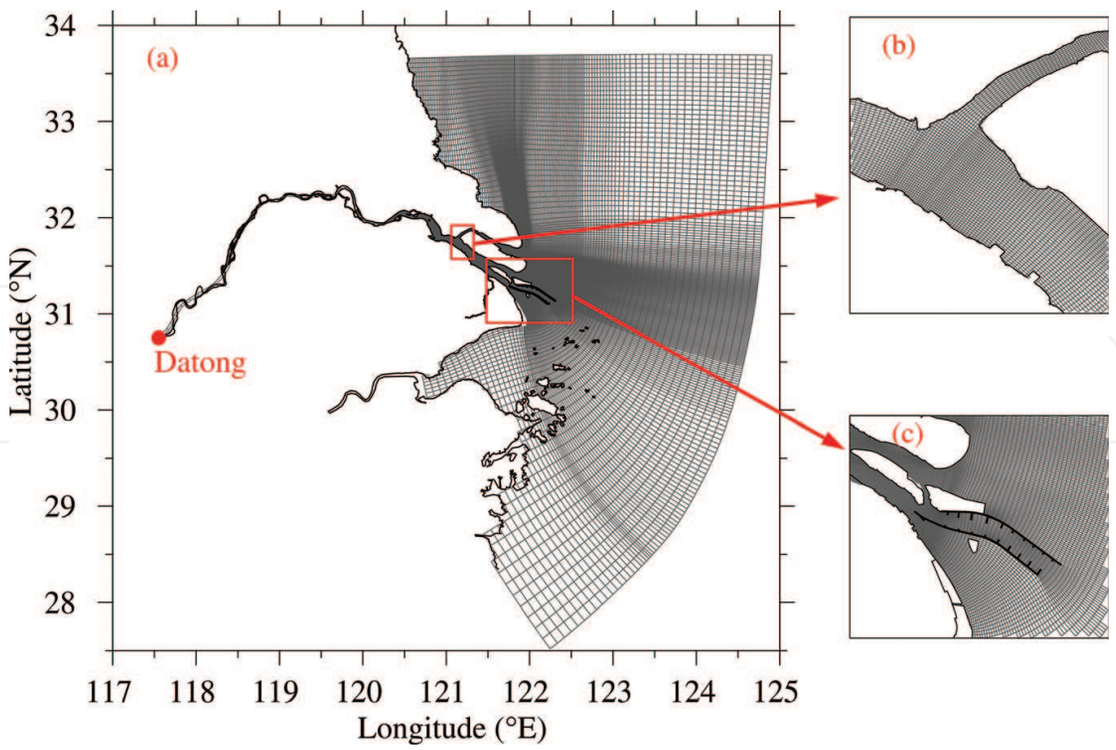

Figure 2. The numerical model mesh (a), an enlarged view of the model mesh around the bifurcation of the NB and the SB (b), and an enlarged view of the model mesh in the NP (c).

The model domain covered the entire Changjiang Estuary, Hangzhou Bay, and adjacent seas from 117.5°E to 125°E and from 27.5°N to 33.7°N (**Figure 2a**). The model was composed of 307 × 224 cells horizontally and 10 uniform σ levels vertically. The horizontal mesh was designed to fit the coastline, with high-resolution grids near the Changjiang mouth, especially near the bifurcation of the SB and NB (**Figure 2b**), and near the NP where a deep waterway was maintained for navigation (**Figure 2c**). A lower-resolution grid was used in open water. The grid resolution ranged from 300 to 600 m in proximity to the river mouth and was 15 km near open water. A wet/dry scheme was included to characterize the intertidal zone due to tidal excursion, and the critical depth was set to 0.2 m.

Derived from the NaoTide dataset (http://www.miz.nao.ac.jp/), the open sea boundary included 16 astronomical constituents: M_2, S_2, N_2, K_2, K_1, O_1, P_1, Q1, MU_2, NU_2, T_2, L_2, $2N_2$, J_1, M_1, and OO_1. The river boundary in the model was specified by the measured daily river discharge at the location of Datong Hydrographic Station, which is 630 km upstream from the river mouth. Wind field used to calculate the sea surface momentum was simulated by the WRF (Weather Research Forecast) Model, or from the observed data of weather station at the Chongming eastern shoal.

The velocities and elevation were initially set to zero. The initial salinity distribution was derived from the Ocean Atlas in the Huanghai Sea and East China Sea (Hydrology) (Editorial Board for Marine Atlas [28]) outside the Changjiang mouth and from observed data inside the river mouth in recent years. Because salinity dominates the density variability in the Changjiang Estuary, water temperature was set to a constant value of 10°C in the model. We have been applying the model in the Changjiang Estuary to study the hydrodynamic processes and saltwater intrusion and have done a lot of work on model validation. The numerical model has been validated many times using data in the Changjiang Estuary, and the results suggest that the model can successfully simulate the hydrodynamic processes and saltwater intrusion in the estuary. A detailed description of the model validation can be found in Wu and Zhu [24], Li et al. [4], and in Qiu and Zhu [12].

3. Dynamic mechanism of saltwater intrusion

The saltwater intrusion in the Changjiang Estuary is controlled mainly by the runoff and tide, but is also influenced by wind, topography, sea level rise, and various projects in the river watersheds and estuary. Using the numerical model described above, we first simulated the saltwater intrusion considering various dynamic factors in a climatological state and then analyzed the impacts of various dynamic factors on the saltwater intrusion using sensitivity experiments.

3.1. Simulation of saltwater intrusion

We considered the monthly mean river discharge and wind in winter to simulate the climatological saltwater intrusion. The river discharge was set at 11,800 m^3/s, which was the mean value measured at Datong Station in January and February from 1950 to 2015. The surface

wind was set to a northerly wind with a constant speed of 5 m/s, which is roughly the mean wind condition in the estuary in winter. The model was run for 60 days from January 1 to March 1, and the analysis was carried out on the outputs of the last spring-neap tidal cycle, or 15 days for salinity spatial distribution, and of the last two spring-neap tidal cycles, or 30 days for temporal variation of salinity at the water intakes of the reservoirs.

To describe the subtidal movement of water in the Changjiang Estuary, we filtered out the tidal current to obtain the residual current during spring and neap tides. In this study, six semidiurnal tidal cycles were used as an averaging time window to remove the semidiurnal and diurnal tidal signals.

The residual water current in the Changjiang Estuary is influenced by several dynamic factors, including runoff, tide, wind, and density gradient. Abundant water discharge drives the residual current to flow seaward, and most is diverted into the SB because of the nearly orthogonal bifurcated channel (**Figure 3**). During spring tide, the surface residual current in the upper reaches of the NB is landward, whereas the residual current is seaward in the middle and lower reaches (**Figure 3a**). Compared to that in the NB, the surface residual current in the SB is much larger. The surface residual currents in the NC, NP, and SP all flow seaward [12].

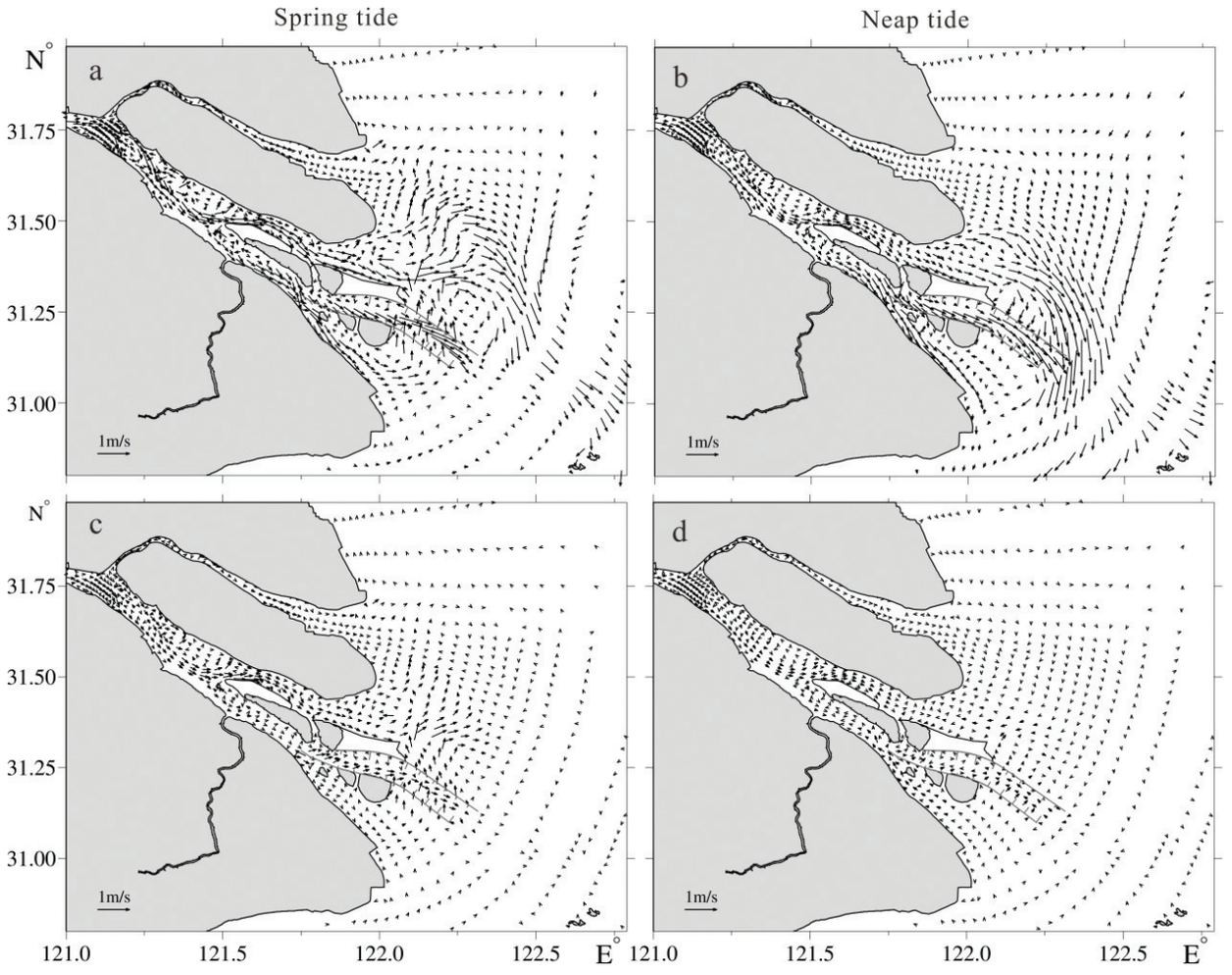

Figure 3. Distribution of residual currents during spring tide (left panel) and neap tide (right panel) under the river discharge of 11,800 m^3/s. (a and b) Surface layer; (c and d) bottom layer.

Moreover, the water overflows across the DWP (Deep Waterway Project) from the SP into the NP and even into the NC, and this acts as one-way transport because the water can cross the dike during flood tide and cannot return to the SP due to the lower elevation during ebb tide. In the bottom layer, the pattern of the residual current is similar with that in the surface layer, but the current is much weaker due to the bottom friction (**Figure 3c**).

During neap tide, the residual current in the surface layer of the upper reaches of the NB is seaward, that is, the net water transport is from the SB into the NB (**Figure 3b**), just opposite of the situation in spring tide. The residual current on the east side of Chongming Island flows eastward and then flows southeastward under the force of northerly wind, rather than flowing northeastward in spring tide, because the wind can easily change the weaker tidal current in neap tide. The overflow across the DWP vanishes in neap tide due to the smaller tidal range. In the bottom layer, the residual currents in neap tide in the SP, middle and lower reaches of the NP, and in the sandbar of the NC are all landward flow because the vertical mixing becomes weaker, which results in stronger landward baroclinic pressure force (**Figure 3d**).

The NB is totally occupied by high-saline water, and the isohaline 5 is close to the bifurcation of the NB and SB. There exist salinity fronts in the upper reaches of the NB, sandbar areas of the NC, NP, and SP (**Figure 4**). At flood slack during spring tide, the saltwater spills over from the NB into the SB, resulting in the water mass with salinity greater than 0.45 appearing in the upper reaches of the SB (**Figure 4a**). As suggested by Wu and Zhu [29], the SSO is mainly caused by the Lagrangian residual and tidal pumping. There exists fresh water in the SB. Around the river mouth, high-salinity water intrudes, and salinity differs among the channels. The distance that isohaline 15 moves upstream in the SP is pronounced compared to that in the NP and is pronounced in the NP compared to that in the NC. The saltwater intrusion in the SP is stronger than that in the NP and is stronger in the NP than that in the NC. In the bottom layer, due to the gravity force, the salinity in the sandbar areas of the NC, NP, and SP is higher

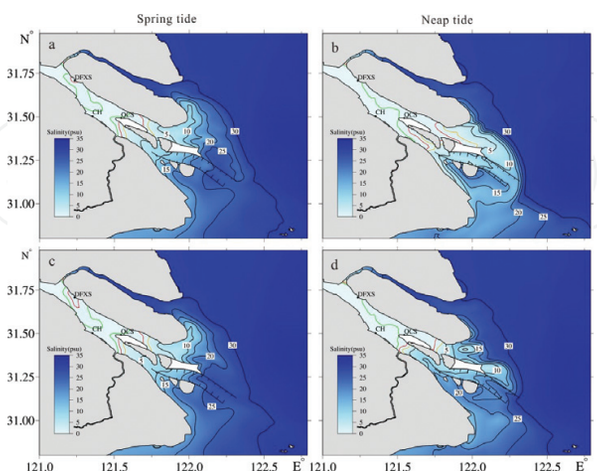

Figure 4. Distribution of salinity at flood slack during spring tide (left panel) and neap tide (right panel) under the river discharge of 11,800 m^3/s. (a and b) Surface layer; (c and d) bottom layer. The green isohalines are 0.45; the red isohalines 1.00; the orange isohalines 2.00; and the black isohalines begin at 5.00 with an interval of 5.00. The reference site of flood slack is Baozhen hydrologic station (red dot, labeled in **Figure 1**), similarly hereinafter.

http://dx.doi.org/10.5772/intechopen.80903

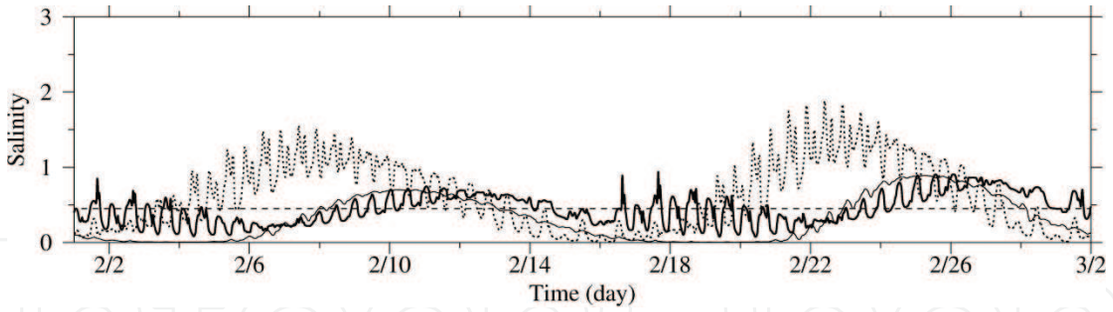

Figure 5. Temporal variation of salinity at the water intakes of the reservoirs under the river discharge of 11,800 m^3/s. Dashed curve: Dongfengxisha reservoir; thin curve: Chenhang reservoir; and thick curve: Qingcaosha reservoir. The horizontal dashed line is the salinity of 0.45, which is the salinity standard of drinking water, similarly hereinafter.

than that in the surface layer (**Figure 4c**). In other water areas, the salinity in the bottom layer is almost the same as that in the surface layer, due to strong vertical mixing in spring tide.

At flood slack during neap tide, the salinity at the upper reaches of the NB becomes lower, and the isohalines extend downstream due to the lower tidal range (**Figure 4b**). There is no SSO; the saline water induced by the SSO in spring tide moves downstream under the runoff force in the SB. Consistent with the change of residual current, the northward extension of the diluted water on the east side of Chongming Island, which appears in spring tide, vanishes, and the distance of eastward freshwater transport in the NC is pronounced. Compared with the saltwater intrusion in the NC, NP, and SP during spring tide, the intrusion becomes weaker in the surface layer due to weaker tide, but becomes stronger in the bottom layer due to weaker vertical mixing and stronger landward baroclinic pressure force and stratification in neap tide.

At present, approximately 70% freshwater supply in Shanghai is taken from the water resources in the Changjiang Estuary. The saltwater intrusion in winter threatens the freshwater safety of the city. There are three reservoirs in the estuary, that is, the QCSR, Chenhang Reservoir, and Dongfengxisha Reservoir (locations marked in **Figure 1**). During saltwater intrusion, the salinity is higher than 0.45 (the salinity standard of drinking water) at water intakes, and the reservoirs can no longer take water from the Changjiang Estuary. Under the river discharge of 11,800 m^3/s during a period of spring-neap tide in February, approximately two-thirds of the time water is taken from the Chenhang Reservoir; approximately half the time, from the Dongfengxisha Reservoir; and more than half the time, from the QCSR (**Figure 5**). Therefore, it is not a problem for the reservoirs in the Changjiang Estuary to receive fresh water from the river to meet the supply demand of drinking water under the climatological mean value of river discharge.

3.2. Impact of river discharge

River discharge is one of the most important dynamic factors determining estuarine saltwater intrusion. The measured river discharge at Datong Station, which accounts for 94.7% of the total river basin discharge, is the upper tidal limit in dry season and is generally used as an

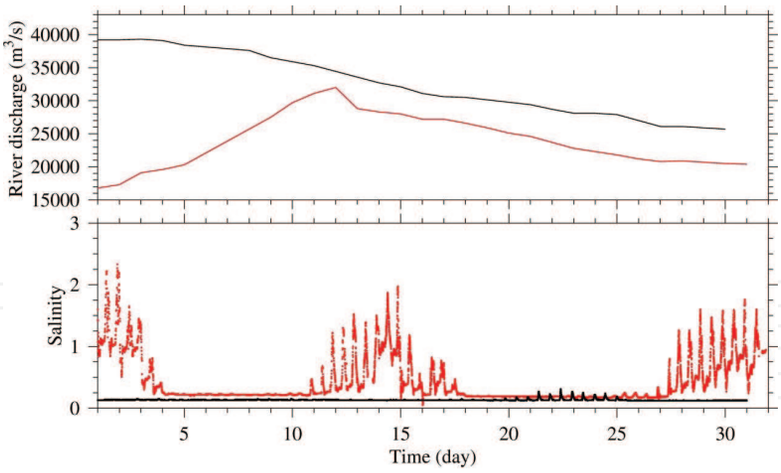

Figure 6. Temporal variation of observed salinity at Chongxi hydrologic station. Red line: March 2009; black line: September 2009.

upper boundary of the estuary in modeling. The river discharge has seasonal variation, which increases from January to July, and then decreases from July to December. The monthly mean river discharge has the minimum of 11,500 m^3/s in January and reaches the maximum of 49,800 m^3/s in July (Changjiang Water Resources Commission, based on the data from 1950 to 2016). The river discharge has interannual variation with higher or lower values in some winters. In this subsection, we analyze the impact of river discharge on the saltwater intrusion based on the measured data and numerical experiments.

The Chongxi Hydrologic Station is located southwest of Chongming Island (red dot in **Figure 1**). The measured salinity shows that the saltwater intrusion was stronger during spring tide, with salinity higher than 1.0 in March 2009 when the river discharge at Datong Station was lower, and the intrusion was very weak in the whole month of September in 2009 when the river discharge at Datong Station was higher (**Figure 6**). Therefore, seasonal variation of river discharge has significant influence on the saltwater intrusion in the estuary.

Salinity at the Chongxi Hydrologic Station was higher during spring tide when the river discharge at Datong Station was lower in April 2009 and was also higher during the first 5 days in April 2010 when the river discharge was close to that in April 2009. In contrast, salinity was much lower, and there was no saltwater intrusion from 6 to 30 in April 2010 when the river discharge was distinctly higher (**Figure 7**). These observational results indicate that annual variation of the river discharge has evident impact on the saltwater intrusion in the estuary.

Besides the numerical experiment with the climatological value of river discharge in January and February, we performed two more experiments with a higher river discharge of 14,000 m^3/s and a lower river discharge of 8000 m^3/s to compare their impacts on the saltwater intrusion. Under the river discharge of 14,000 m^3/s, the salinity in the upper reaches of the NB is obviously decreased (**Figure 8**); there is no saline water with salinity greater than 0.45 in the SB, that is, no SSO occurs. At flood slack during spring and neap tides, there is fresh water in both surface and bottom layers at the three water intakes of the reservoirs. Compared with the results under the river discharge of 11,800 m^3/s, the isohalines near the river mouth under the

http://dx.doi.org/10.5772/intechopen.80903

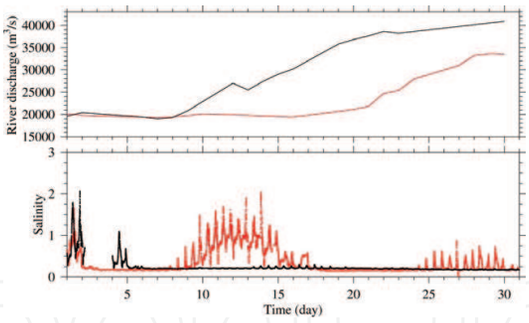

Figure 7. Temporal variation of observed salinity at Chongxi hydrologic station. Red line: April 2009; black line: April 2010.

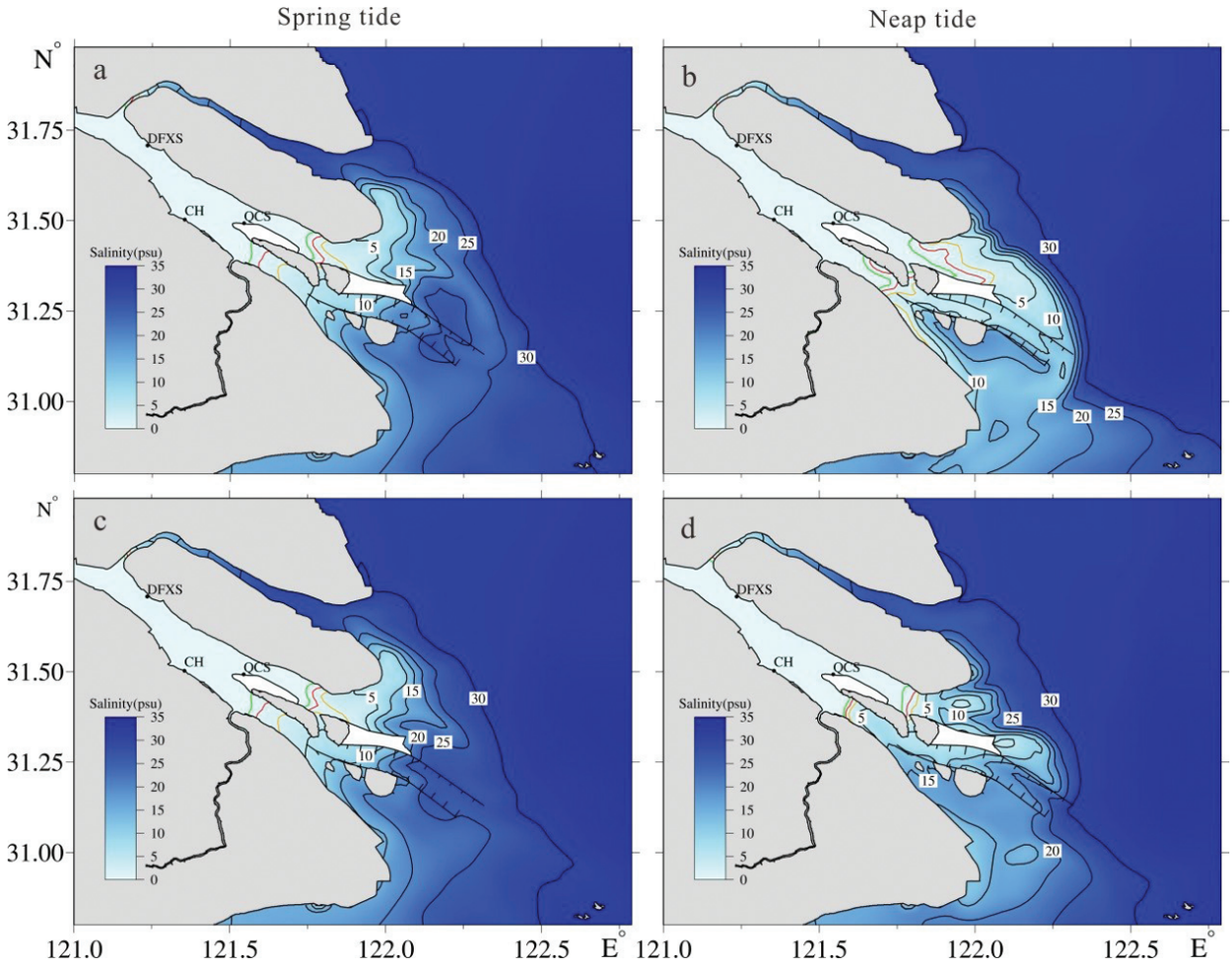

Figure 8. Distribution of salinity at flood slack during spring tide (left panel) and neap tide (right panel) under the river discharge of 14,000 m^3/s. (a and b) Surface layer; (c and d): bottom layer.

river discharge of 14,000 m^3/s move downstream distinctly, indicating that the saltwater intrusion is weakened due to larger river discharge. In spring tide, more diluted water is transported from the NC into the NB (**Figure 8a** and **c**). Compared with the locations of the isohalines in spring tide, the isohalines of 0.45 in the NC and SC move downstream in neap

tide (**Figure 8b** and **d**), meaning that the saltwater intrusion in neap tide is weaker than that in spring tide.

Under a larger river discharge of 14,000 m^3/s, the salinity during a period of spring-neap tides in February at the water intakes of the Qingcaosha and Chenhang reservoirs is lower than 0.45 at any time, that is, there is no saltwater intrusion influencing the water intakes of the two reservoirs (**Figure 9**). Approximately, two-thirds of the time the salinity at the water intake of the Dongfengxisha Reservoir is lower than 0.45. Therefore, there is sufficient time for the reservoirs to take fresh water from the river when the river discharge is larger.

Under the lower river discharge of 8000 m^3/s, the salinity in the upper reaches of the NB is obviously increased (**Figure 10**). There is saline water with salinity greater than 1.0 in the SB, that is, SSO becomes stronger. At flood slack during spring and neap tides, there is no fresh water in both surface and bottom layers at the three water intakes of the reservoirs. Compared with results under the river discharge of 11,800 m^3/s, the isohalines near the river mouth move upstream clearly, indicating that the saltwater intrusion is enhanced due to the lower river discharge. Compared with the locations of the isohalines in spring tide, the isohaline 5 in the NC and the SC moves downstream in neap tide, meaning that the saltwater intrusion in neap tide is weaker than that in spring tide. Salinity is higher than 20 in most areas of the SP, that is, the saltwater intrusion there is very strong.

Under the lower river discharge of 8000 m^3/s during a period of spring-neap tides in February, fresh water can be taken from the river approximately one-thirds of the time for the Dongfengxisha Reservoir, half the time for the Chenhang Reservoir, and shorter time for the QCSR (**Figure 11**). Therefore, there is less time for the reservoirs to take fresh water from the river when the river discharge is lower.

Based on the analyses of observed data and numerical experiments, we can conclude that the effect of river discharge on the saltwater intrusion in the Changjiang Estuary is significant. When the river discharge decreases, SSO and saltwater intrusion are enhanced in each channel.

3.3. Impact of tide

The tides in the estuary exhibit semidiurnal, diurnal and fortnightly spring-neap signals [5, 25]. The tide is medium with mean tidal range of 2.66 m at the mouth, and is the most energetic

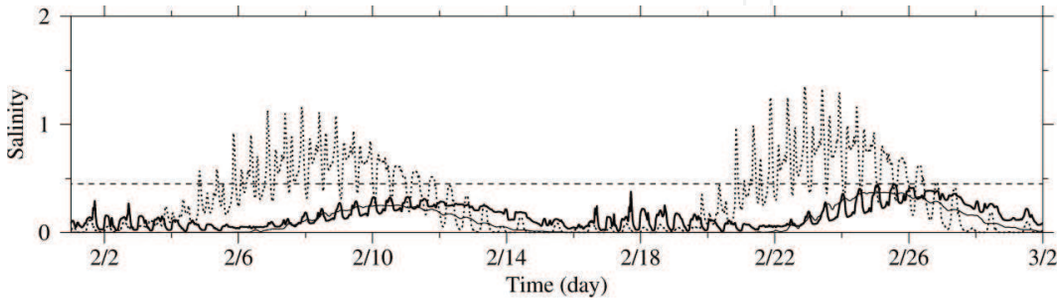

Figure 9. Temporal variation of salinity at the water intakes of the reservoirs under the river discharge of 14,000 m^3/s. Dashed curve: Dongfengxisha reservoir; thin curve: Chenhang reservoir; and thick curve: Qingcaosha reservoir.

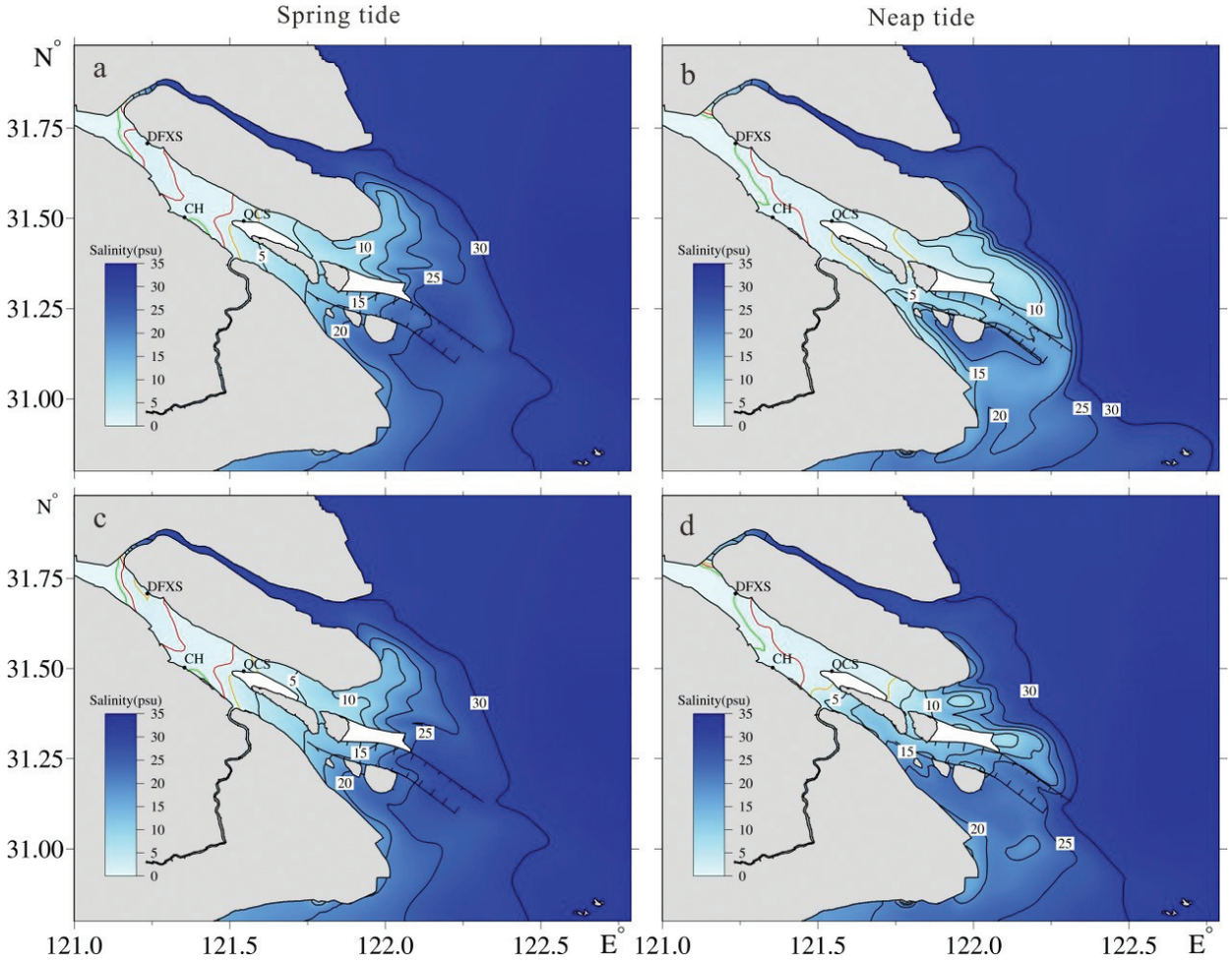

Figure 10. Distribution of salinity at flood slack during spring tide (left panel) and neap tide (right panel) under the river discharge of 8000 m^3/s. (a and b) Surface layer; (c and d) bottom layer.

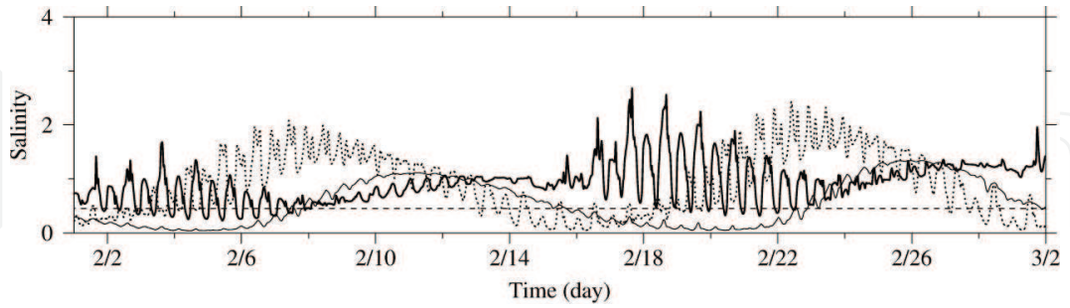

Figure 11. Temporal variation of salinity at the water intakes of the reservoirs under the river discharge of 8000 m^3/s. Dashed curve: Dongfengxisha reservoir; thin curve: Chenhang reservoir; and thick curve: Qingcaosha reservoir.

source of water movement in the Changjiang Estuary. On the intertidal timescales, the semidiurnal tide drives saltwater into the estuary during flood tide and out of the estuary during ebb tide. The fortnightly spring tide generates a greater saltwater intrusion than the neap tide does. The saltwater intrusion is also enhanced by the seasonal variability of tides, with the maximum tidal range in March [8, 25].

The results of numerical experiments in Subsections 3.2 and 3.3 clearly show that the saltwater intrusion in spring tide is stronger than that in neap tide. In this subsection, we further analyze the impact of tide on saltwater intrusion based on the observed data. We conducted an observation in the SP in January 2010 and selected one measured site located in the upper reaches of the SP to illustrate the variation of currents and salinity with tides (**Figure 12**). The observed data show that the current was a rectilinear current inside the river mouth rather than a rotational current as that outside the river mouth. The current speed was larger in the spring tide than in the neap tide. The current speed in the surface layer was larger than that in the bottom layer due to the bottom friction. The current duration in ebb current was longer than that in flood current. The salinity in the surface layer was higher than that in the bottom layer. The semidiurnal and fortnightly variations of salinity were evident, which were certainly caused by tides.

The observed salinity at the Chongxi Hydrological Station in January 2010 also distinctly shows semidiurnal and fortnightly variations with tides (**Figure 13**). Therefore, tides are one of the important dynamic factors determining the saltwater intrusion in the estuary.

3.4. Impact of wind

Wind over the Changjiang Estuary is primarily the monsoon, which is weak southerly in summer and strong northerly in winter. Li et al. [4] studied the impact of wind on the saltwater intrusion in the Changjiang Estuary. The observation at the Chongxi Hydrologic Station indicated the salinity increased abnormally during strong northerly wind. It was confirmed

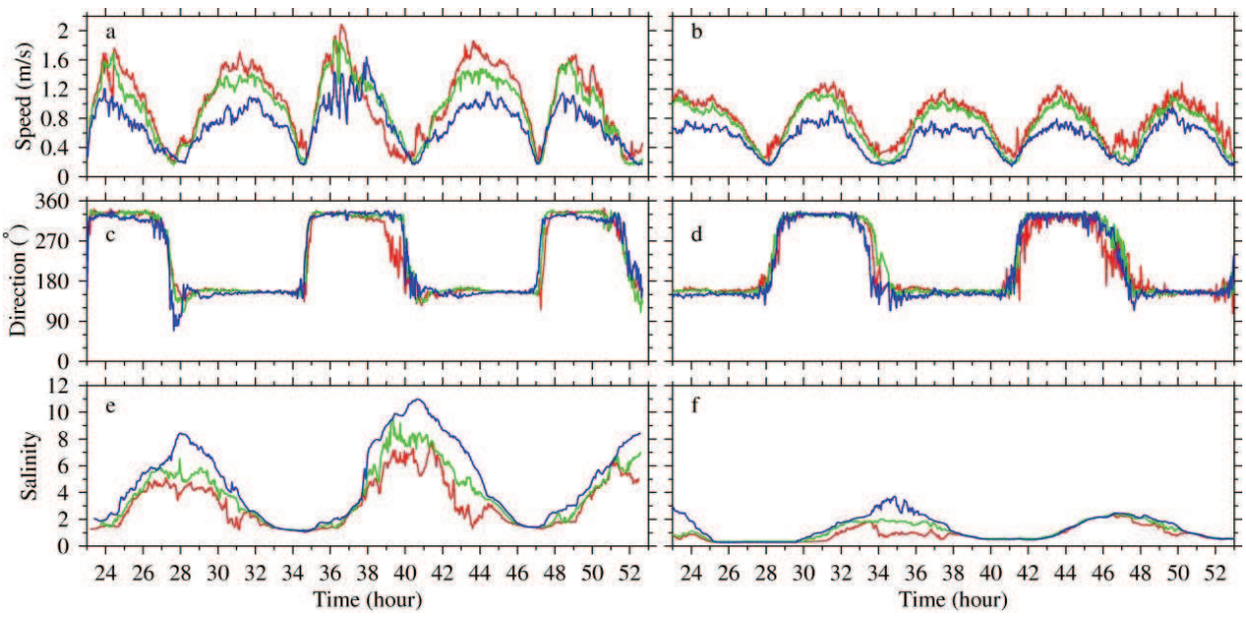

Figure 12. Temporal variations of observed current speed (upper), current direction (middle), and salinity (lower) at the upper reaches of the SP during spring tide (left panel, from 23:00 on January 18 to 5:00 on January 20, 2010) and the neap tide (right panel, from 23:00 on January 25 to 5:00 on January 27, 2010). Red line: surface layer; green line: middle layer; and purple line: bottom layer.

http://dx.doi.org/10.5772/intechopen.80903

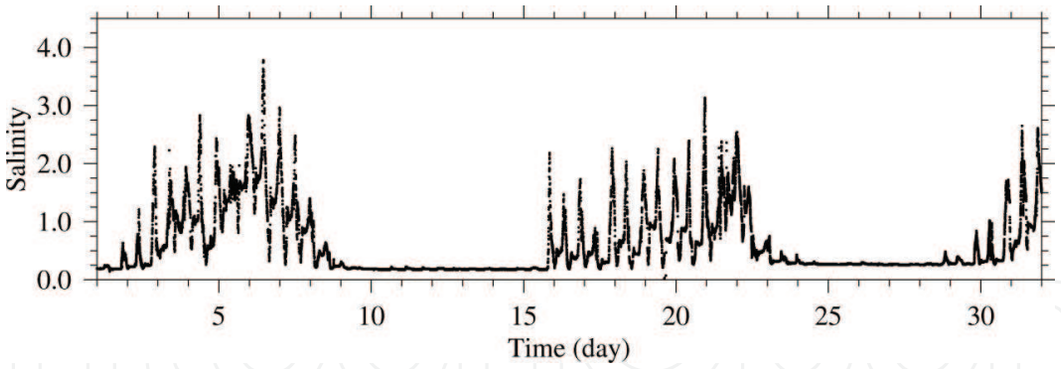

Figure 13. Temporal variation of observed salinity at Chongxi hydrological station in January 2010.

that the abnormal increments of salinity at the Chongxi Hydrologic Station during the neap and moderate tides were caused by strong northerly wind.

Numerical experiments were carried out to study the effects of different wind speeds and directions on wind-driven currents and saltwater intrusion. In the control experiment, the river boundary was specified using a discharge of 11,000 m^3/s, which was roughly the monthly averaged value in January and February; wind was set to the northerly wind of 5 m/s, which represented the general wind condition in January and February. Two additional numerical experiments were run without wind (Experiment A) or with stronger northerly wind of 10 m/s (Experiment B), to represent weaker and stronger wind stress cases. In addition, two more experiments with a northeasterly wind of 5 m/s (Experiment C) and a northwesterly wind of 5 m/s (Experiment D) were conducted to explore the effect of wind direction on the saltwater intrusion.

When driven by the northerly wind of 5 m/s, southward currents along the Subei Coast formed and landward Ekman transport appeared due to the Coriolis force (**Figure 14a**). In the lower reaches of the NB, the wind-driven circulation was landward on the north side and seaward on the south side to ensure the mass conservation. In the SC and NC, a significant horizontal circulation is formed, which flowed landward in the NC and seaward in the SC. In the SP and NP, this circulation was seaward. Such patterns of wind-driven circulation can increase the flood current and decrease the ebb/net water current in the NC, thereby restricting the extension of the fresher water there and weakening the saltwater intrusion in the SC, SP, and NP. In addition, the wind-induced circulation in the upper and middle reaches of the NB flowed into the SB and discharged seaward in the upper reaches of the SB [4].

The difference of depth-averaged salinity between Experiment A (no wind) and the control experiment during spring tide is shown in **Figure 15a**. In Experiment A, because there is no wind-driven southward current along the coast and the landward Ekman water transports, the salinity in the mouth of the NB was significantly decreased by 3–10, and decreased by 1 off the SP and NP. In addition, without considering the wind-driven circulation, the saltwater intrusion in the upper reaches of the NB was weakened with salinity decreasing by 1–5, and the intensity of SSO was abated, which caused a slight decrease of salinity in the SB. Without the effects of wind-driven circulation in the SC and NC, the saltwater intrusion in the NC was

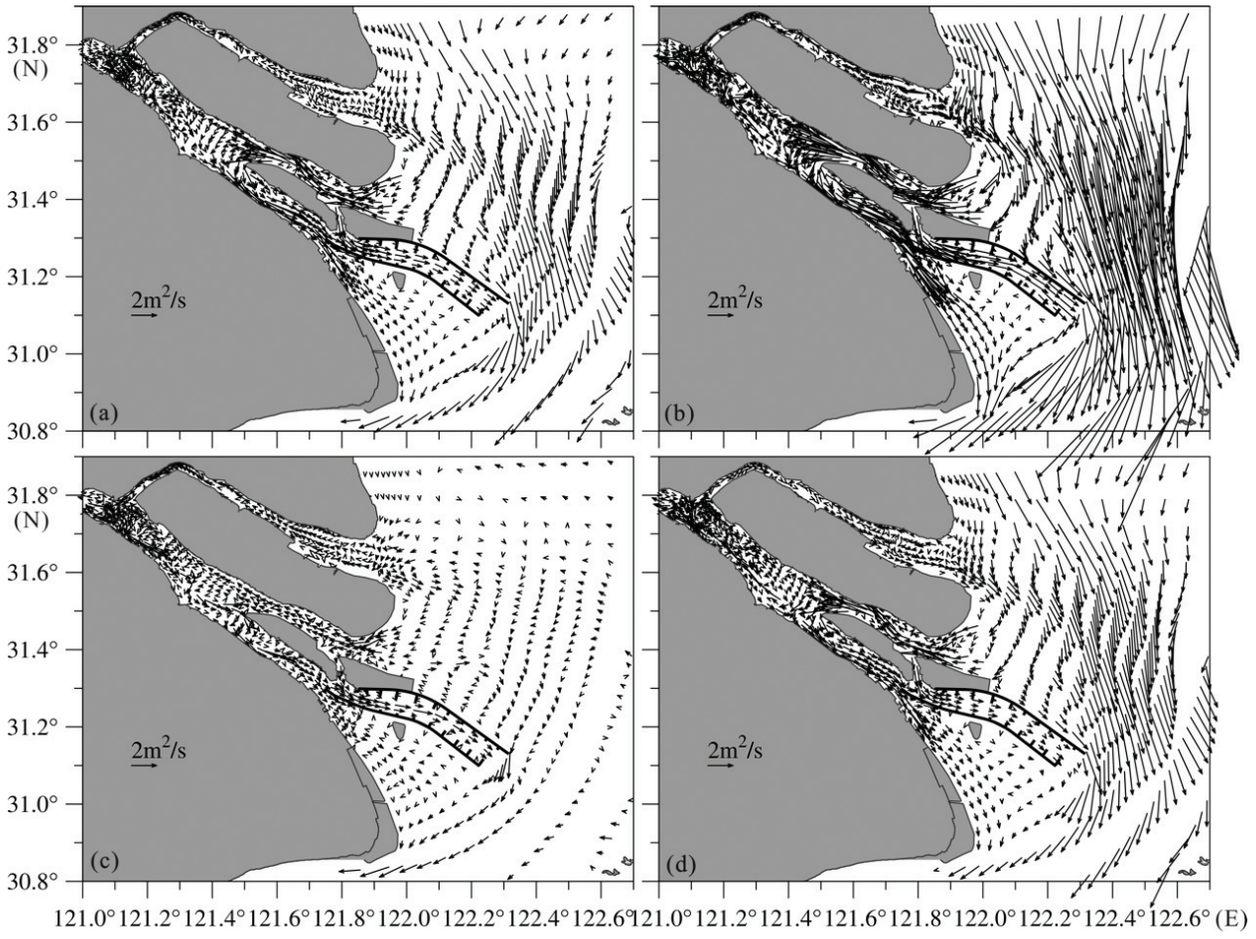

Figure 14. Pure wind-driven net unit width water flux under the northerly wind of 5 m/s (a), the northerly wind of 10 m/s (b), the northeasterly wind of 5 m/s (c), and northwesterly wind of 5 m/s (d).

weakened with salinity decreasing by 0.2–1.0, whereas that in the SC, SP, and NP was enhanced with salinity increasing by 1–3. During neap tide, there was larger variation of salinity in the mouth of the NB, the eastern of the Chongming Island and the SP compared to that during spring tide (not shown) [4].

The wind-driven current was enhanced greatly by the northerly wind of 10 m/s, but the current pattern remained the same as that in the control experiment (**Figure 14b**). Under the interaction of river discharge and tide, when including the northerly wind of 10 m/s (Experiment B), the wind driven circulation during the spring tide off the Changjiang Estuary brought more seawater to the mouth, and the salinity off the NB increased by 1–5 compared to the control experiment. The salinity in the upper reaches of the NB increased by 5 and thereby enhanced the SSO, which further increased the salinity with a range of 1–2 in the SB. The salinity in the east of Chongming Island increased by more than 20, and the saltwater intrusion was pronounced in the NC with salinity increase of 5–20. The salinity in the SC increased by ~1, which was due to the stronger SSO. The saltwater intrusion in the SP and NP were weakened, and the salinity decreased by a maximum value of 5 in the SP. During neap tide (not shown), the difference of salinity in the NC and SP was more significant compared to that during spring tide, whereas it was almost the same in the rest of the study area [4].

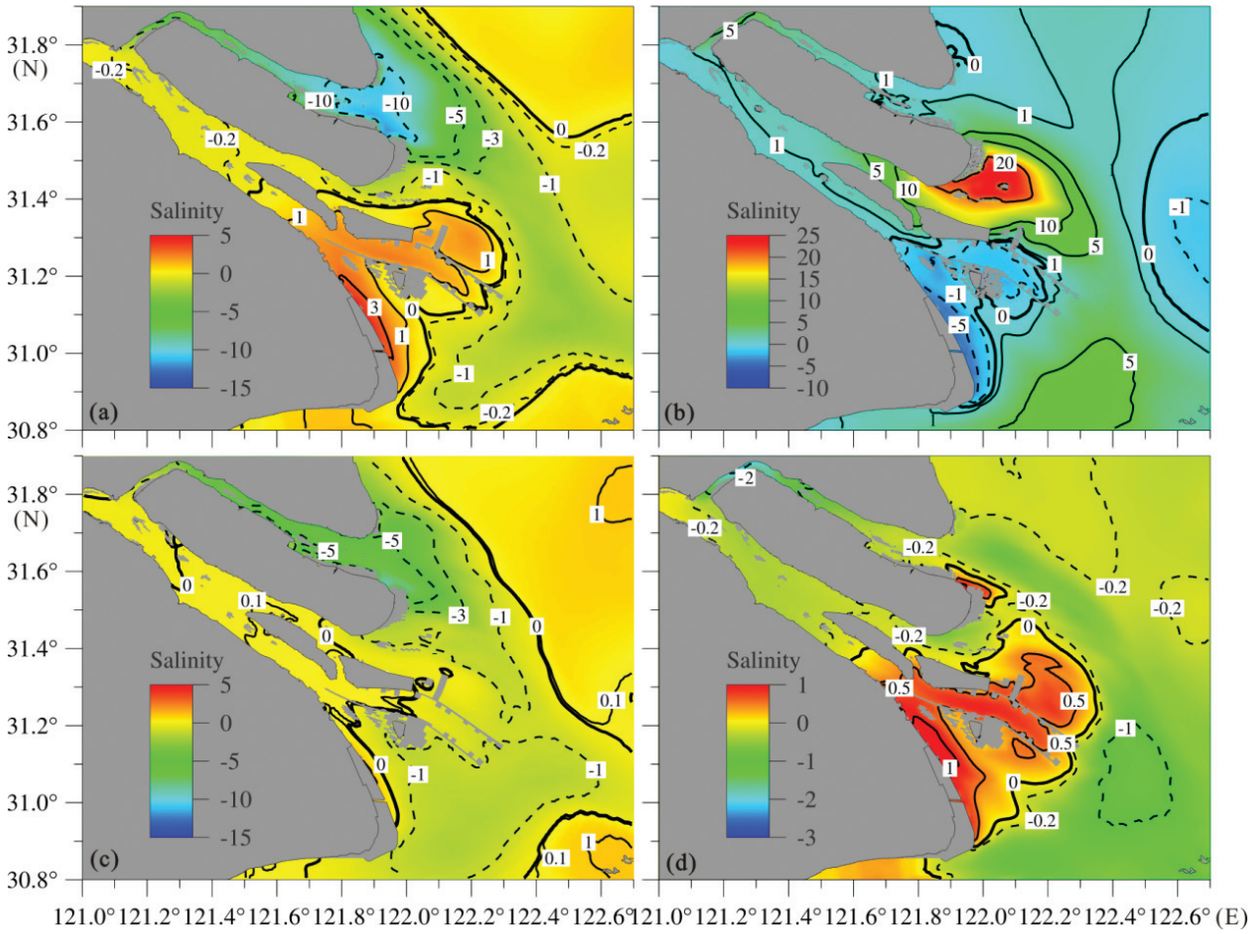

Figure 15. Salinity difference distribution of depth-averaged salinity in experiment a (a), experiment B (b), experiment C (c), and experiment D (d) with respect to depth-averaged salinity in the control experiment during spring tide. Zero contour is bold, solid contours denote positive values, and dashed ones denote negative values.

When driven by the northeasterly wind of 5 m/s, the wind-driven circulation in the lower reaches of the NB as well as that in the SC and NC was significantly weakened (**Figure 14c**). Under the interaction of river discharge and tide, when including the northeasterly wind of 5 m/s (Experiment C), a weaker saltwater intrusion in the NB was detected during the spring tide (**Figure 15c**), compared to the control experiment, and their difference was more than 5 at the mouth and decreased gradually to 1 in the upper reaches. The salinity at the mouth of the NC decreased by 1–3, while it decreased by ~1 in the middle and lower reaches of the NP and SP, and in the areas off the SP and NP. In addition, the salinity in most areas of the SB, the upper reaches of NC, the SC, and the upper reaches of the NP is similar to that in the control experiment. In Experiment C, the relatively weak circulation in the NC led to fresher water there exchanging with the high-saline water off the NB and further decreased the salinity in the NB with strong tide [4].

When driven by the northwesterly wind of 5 m/s, the features of wind-driven circulation in the SC and NC are similar to those under the northerly wind of 5 m/s. Along the southeast-ward channel in the middle and lower reaches of the NB, the seaward water transport driven by local wind stress is greater than that induced by landward Ekman transport, and the wind-driven

circulation was from the SB to the NB (**Figure 14d**) to ensure the continuity of water mass [4]. Under the interaction of river discharge and tide, when including the northwesterly wind of 5 m/s (Experiment D), the salinity in the middle and lower reaches of the NB decreased by 0.2 during spring tide (**Figure 15d**), while it decreased by 2 in the upper reaches. The local effects of the northwesterly wind in the middle and lower reaches of the NB restrict flood tidal currents, and thereby weaken the saltwater intrusion in this channel. The salinity decreased by 0.2 in the middle and upper reaches of the SB and in the upper reaches of NC, while it increased by 0.5 in the mouth of the NC, SP, and NP [4].

3.5. Impact of sea level rise

Global sea level rise has been of great concern by governments and societies with its impacts on saltwater intrusion and material transports in estuaries, which threaten freshwater habitats and drinking water supplies. Sea level rise deepens water depth and changes currents and saltwater intrusion in estuaries. Qiu and Zhu [13] simulated the variations of saltwater intrusion according to different sea level rise scenarios in a typical year and a dry year. Three sea level rise scenarios were considered. Scenario 1: 2.90 mm/a, total sea level rise around 0.290 m in future 100 years; Scenario 2: 4.83 mm/a, total sea level rise around 0.483 m in future 100 years; and Scenario 3: 10.00 mm/a, total sea level rise around 1.000 m in future 100 years. The river discharge record from 1990 to 2013 at Datong Station showed that a severe drought occurred in January 1999, with an average discharge of 9480 m^3/s, while the discharge is 13,463 m^3/s in the same month of 2012, which was a typical year. The saltwater intrusion generally occurs from the mid-December and keeps on influencing the Changjiang Estuary until the following March. The river discharge reduces to its minimal value in January, during which the saltwater can intrude farther upstream and the saltwater intrusion becomes the most serious in the whole year. Thus, the period of model simulation was set from October to the following May to present the whole process of saltwater intrusion and focus on the monthly mean salinity during January. The river discharges from 1998 to 1999 (dry year) and from 2011 to 2012 (typical year) were used [13].

To evaluate the influence of sea level rise on the saltwater intrusion in the Changjiang Estuary, both present-day sea level and future scenarios with sea level rise were used in the simulations. In the base case, the model results for the dry year and typical year were simulated by using the present-day sea level. In each sea level rise scenario, the increased sea level was added to the mean sea level used in the base case. We named the cases as Experiment S1, S2, and S3 to indicate the situations after sea level rising by 0.290, 0.483 and 1.00 m, respectively [13]. All other set-ups in these cases were identical to the base case.

In a dry year, the saltwater near the river mouth intrudes more landward than that in a typical year, and the distance that isohaline 1 moves upstream in the upper NC and the SC is distinctly farther (**Figure 16a** and **b**). The NB is generally occupied by saline water in both dry and typical years, while the SSO is pronounced in a dry year due to the lower river discharge [13].

Figure 16C–H shows pronounced variation, that is, salt content increases obviously as sea level rises in both dry year and typical year. Due to the difference of river discharge, the change

http://dx.doi.org/10.5772/intechopen.80903

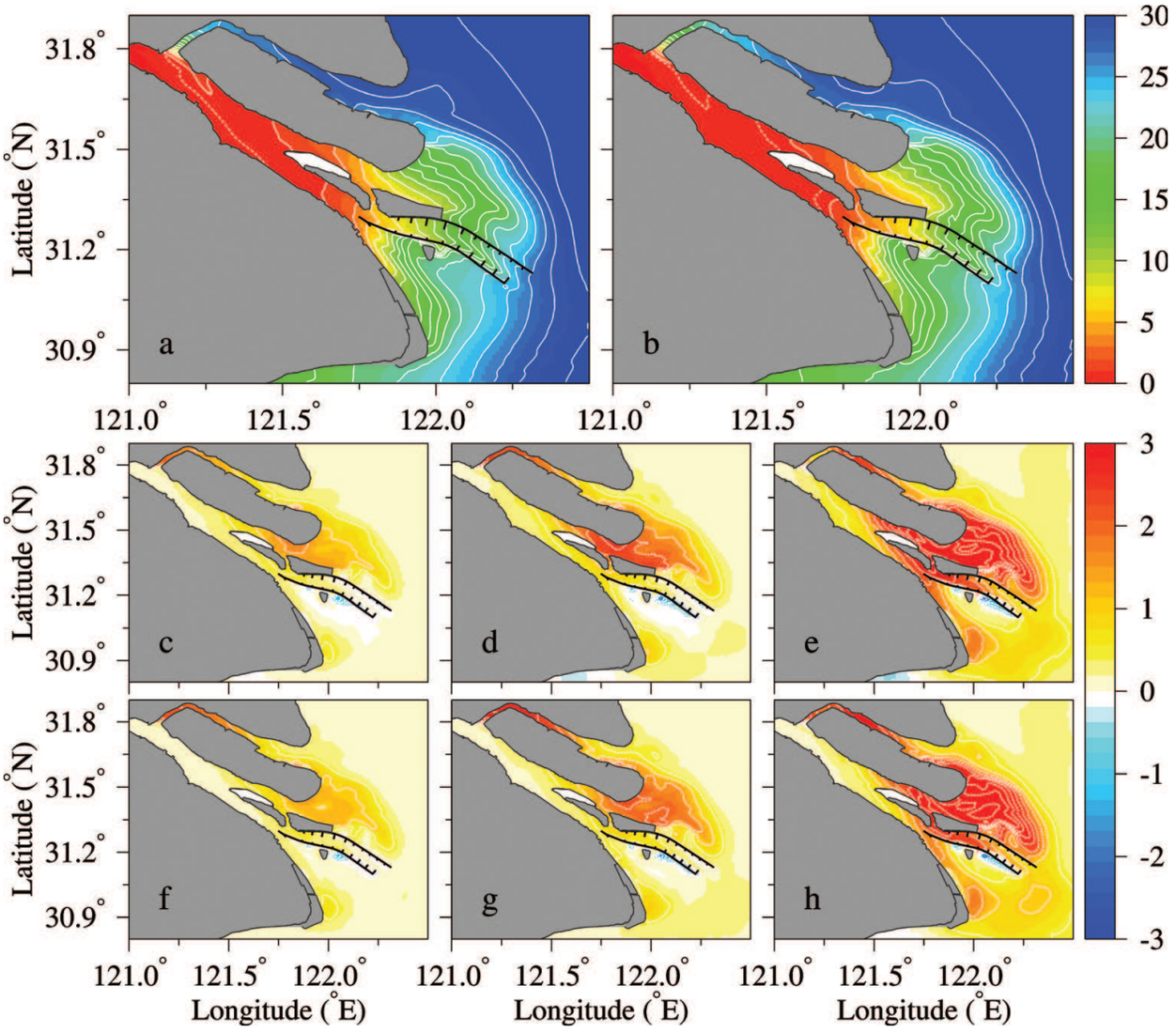

Figure 16. Distributions of depth-averaged salinity in the base case in dry year (a) and typical year (b), respectively. White lines indicate the salinity isohalines from 1 to 31 with an increment of 2, and the dashed lines indicate the isohaline of 0.5. (c–h) Distributions of depth-averaged salinity difference in numerical experiments S1, S2, and S3 with respect to the base case during January in dry year (c, d, e) and typical year (f, g, h), respectively. White lines indicate the salinity difference isohalines with an interval of 0.50. All the results are monthly mean in January in the corresponding year [13].

of saltwater intrusion has an interannual variation, namely, the salinity increase in the NC, NP, and SP is larger in a dry year than that in a typical year as sea level rises. However, because the salt content in the NB is higher in a dry year than in a typical year in the base case (**Figure 16a** and **b**), salinity increase is lower in a dry year in all sea level rise scenarios. Wu et al. [2] showed a relationship between runoff and semi-monthly water flux in the upper NB, which suggests that the SSO may impact the SB more severely under a lower river discharge. The SSO, together with the enhanced saltwater intrusion from the NC, increases the salt content in the upper SB in both dry and typical years with rising sea level (**Figure 16C–H**). Under the lower river discharge, the salinity increase in a dry year is more pronounced in the upper SB as sea level rises, and the enhanced SSO is one of the important factors for this

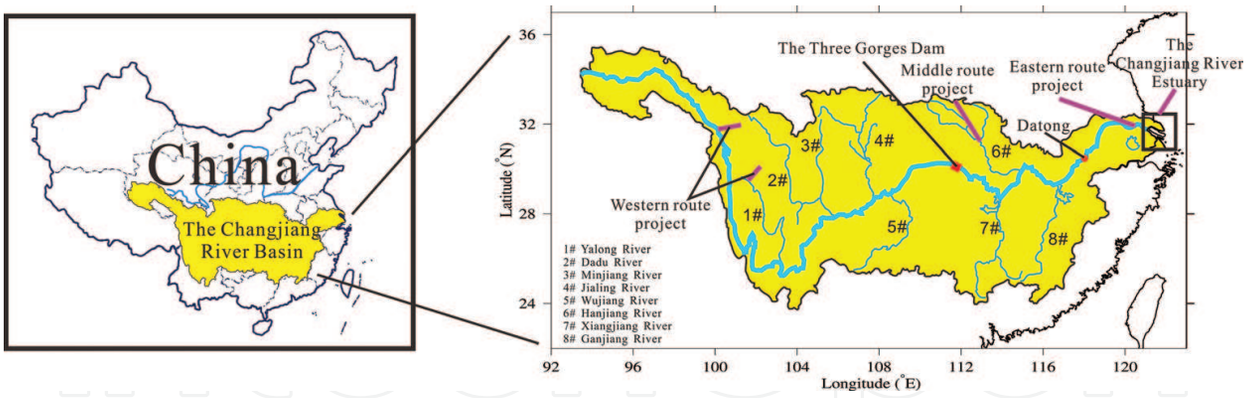

Figure 17. Sketch of the Changjiang Basin and the locations of the Three Gorges Project and Water Diversion South to the North Project.

increase [13]. Then, the increased SSO will move downstream under runoff and impact the lower reaches.

3.6. Impact of major projects in the river basin and estuary

There have been many man-made projects in the river basin and estuary. In this subsection, we consider the impacts of one major project in the estuary and two major projects in the river basin on the saltwater intrusion. The three projects are the DWP in the estuary (labeled in **Figure 1**), the Three Gorges Dam (TGD), and the Water Diversion South to the North Project (WDP) (**Figure 17**).

Zhu et al. [10] analyzed the impact of the DWP on the saltwater intrusion in the Changjiang Estuary. In the NC, the saltwater intrusion was alleviated distinctly after the DWP, because the dykes of the project blocked off the southward drift of the brackish water plume under the northerly monsoon and the Coriolis force. The saltwater intrusion in the project area was intensified at the upper section and alleviated at the lower section. In the SP, the saltwater intrusion was intensified as the background salinity increased and the river discharge decreased. The DWP had an obvious impact on the saltwater intrusion in the Changjiang Estuary [10].

The TGD is the largest water conservancy project in the world. It significantly regulates the discharge of the Changjiang on a seasonal scale [10]. It stores water in autumn and releases it during the following dry season. Qiu and Zhu [12] used the numerical model to simulate the seasonal saltwater intrusion around the Changjiang Estuary under the scenarios with and without the TGD regulation. The seaward residual water transport was augmented during the dry season after the TGD began operating, which means that more fresh water was discharged into the sea, resulting in a weaker saltwater intrusion in each channel. During spring tide (**Figure 18a**), the salinity generally decreased in the estuary. The net water flux increased in the NB and diluted the high-salinity water in its upper reaches [12]. This led to a decline in the salt flux that spilled over into the SB. Around the river mouth, the salinity in the NP and SP generally decreased to about 1. In the NC, the salinity also decreased. During neap tide (not shown), the salinity difference reached −2.5 in the upper

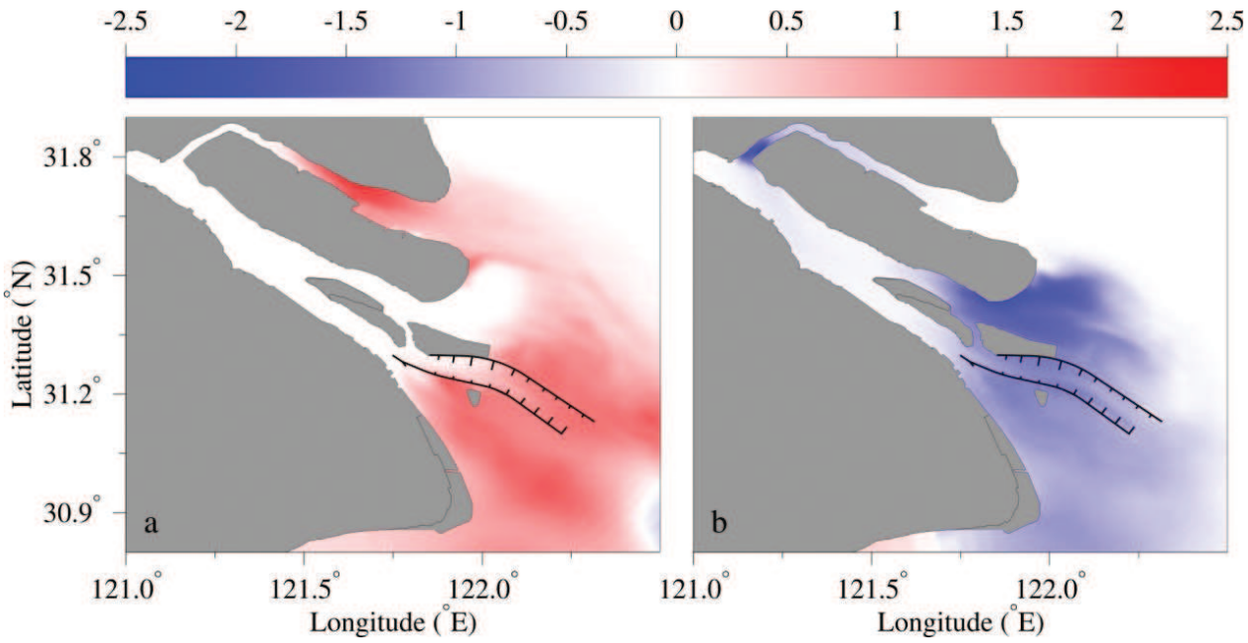

Figure 18. Tidally averaged surface salinity difference between after and before the project during spring tide. (a) TGR; (b) eastern WDP. A positive value means salinity increase after the projects and the negative value indicates salinity decrease after the projects.

NB that was mainly caused by the seaward movement of the salinity front. The value of salinity difference was about 1 in the SP and NP, and it decreased slightly in the NC. These results showed that as the TGD supplemented river discharge during the dry season, the saltwater intrusion was suppressed. They also showed that the operation of the TGD was favorable for reducing the burden of freshwater supplement in the highly populated estuarine region.

The WDP is a strategic project to ease the shortage of water resources in northern China. China has been enduring floods in the south and droughts in the north. The water resources will be reallocated by the WDP through the inter-basin water transfer to mitigate the shortage of water resources in northern China. The WDP has three water transfer plans, namely, the Western Route Project, Middle Route Project, and Eastern Route Project. The Eastern Route Project draws water from Yangzhou, which is in the lower reaches of the Changjiang, and conveys the drawn water to northern China through the Grand Canal and the parallel rivers. Two numerical experiments before and after the eastern WDP were set up with the monthly mean river discharge of 11,200 m^3/s in January, and 10,400 m^3/s (reduced by 800 m^3/s due to the third phase eastern WDP), respectively. The eastern WDP caused a decrease of river discharge, resulting in an enhancement of the saltwater intrusion, especially around the sand bars at the river mouth where the salinity experienced a notable increase. This project enhanced the SSO and increased the net seaward salt flux in the SB. During spring tide (**Figure 18b**), the salinity in the upper SB was mainly affected by the SSO, while that around the sand bars at the river mouth where the salinity fronts existed was mainly impacted by the seawater intrusion. During neap tide (not shown), the saltwater intrusion was weaker due to weaker tides. Accordingly, the SSO was much weaker and had a weaker effect on the salinity in the upper

SB. After the eastern WDP, the enhancement of the saltwater intrusion during neap tide was weaker in the NC and greater in the SP and the NP, compared to that during spring tide.

4. Summary

The Changjiang is one of the largest rivers in the world, with three bifurcations and four outlets into the sea. Its discharge exhibits pronounced seasonal variation, with the lowest monthly mean value of 11,200 $m^3 s^{-1}$ in January and the highest of 49,700 $m^3 s^{-1}$ in July. The tide has semidiurnal, diurnal, and fortnightly spring-neap signals with a moderate tidal range. Winds are controlled primarily by the monsoon, which brings weaker southerly wind in summer and stronger northerly wind in winter. There is a net landward flow in the NB when river discharge is low during spring tide, resulting in a type of saltwater intrusion known as the SSO, which is the most striking characteristic of saltwater intrusion in the estuary.

A three-dimensional numerical model was developed to study the hydrodynamic processes and saltwater intrusion in the Changjiang Estuary. A third-order spatial interpolation at a moderate temporal resolution coupled with a TVD limiter (HSIMT-TVD) advection scheme was used in this model to solve the transport equation and prevent numerical oscillations. The model was validated many times in the Changjiang Estuary, and the results suggested that the model can successfully simulate the hydrodynamic processes and saltwater intrusion in the estuary.

With combined effect of river discharge, tide, wind, and baroclinic force induced by the density gradient, the simulated winter residual currents during spring tide in the SB, SC, NC, and NP flow seaward mainly due to the runoff and have a higher magnitude in these channels than over the tidal flats. In the sandbar areas between the SP and NP, water is transported northward across the tidal flats. The residual current over the tidal flat east of Chongming Island is northward. In the NB, the residual current is weaker, and there is a net water transport toward the SB.

The saltwater intrusion in the Changjiang Estuary is controlled mainly by river discharge and tide, but is also influenced by wind, sea level rise, river basin, and estuary projects. The saltwater intrusion is enhanced when river discharge decreases. There is sufficient time for the reservoirs to take fresh water from the river when river discharge is large. On the intertidal timescale, the semidiurnal tide drives saltwater into the estuary during flood tide and out of the estuary during ebb tide. The fortnightly spring tide generates a greater saltwater intrusion than during neap tide. The model reproduced the phenomenon of SSO. The saltwater intrusion in the SP is stronger than that in the NP, and the intrusion in the NP is stronger than that in the NC.

Considering wind, sea level rise, and major projects in the river basin and estuary, we simulated and analyzed their impacts on the saltwater intrusion in the Changjiang Estuary. The northerly wind produced southward currents along the Subei Coast as well as the landward Ekman transport, which brought seawater into the Changjiang Estuary. A significant horizontal wind-driven circulation was formed in the SC and NC, which flowed landward in the NC

and seaward in the SC, SP, and NP. The saltwater intrusion was enhanced by the landward circulation, while it was weakened by the seaward circulation. With increasing northerly wind speed, the saltwater intrusion was enhanced in the NB and NC, while it was weakened in the SC, SP, and NP. When driven by the northeasterly wind, the wind-driven circulation in the SC and NC was significantly decreased, and the saltwater intrusion was weakened in the NB and NC compared to the same speed of northerly wind. In the upper reaches of the NB, the water was directly dragged by the local wind, causing an increment of water spilling over the flats from the NB into the SB. However, the SSO was weakened during spring tide, because the fresher water extended from the NC into the NB was more pronounced. When driven by the northwesterly wind, the patterns of the wind-driven circulation in the SC and NC were almost the same as those driven by the northerly wind of the same speed. In the middle and lower reaches of the NB, the water was directly dragged by the local wind, causing a weakened saltwater intrusion there, which decreased the salinity in the upper reaches of the NB and weakened the SSO. The saltwater intrusion was slightly weakened in the upper reaches of the SB and NC and was enhanced in the mouth of the NC, SP, and NP. The influence of wind stress was more pronounced during neap tide than during spring tide. The river discharge and tide mainly determined the features of the saltwater intrusion in the Changjiang Estuary, though the wind also played a key role.

The saltwater intrusion becomes stronger as sea level rises and is much stronger when river discharge is much smaller. The SSO, together with the enhanced saltwater intrusion from the NC, increases the salt content in the upper SB with the rising sea level. Under a lower river discharge, the salinity increase in dry year is more pronounced in the upper SB as the sea level rises, and the enhanced SSO is one of the important factors for such increase.

The impact of the DWP is that the saltwater intrusion was alleviated distinctly in the NC because the dykes of the project blocked off the southward drift of the brackish water plume under the northerly monsoon and the Coriolis force. The saltwater intrusion in the NP was intensified at the upper section and alleviated at the lower section. In the SP, the saltwater intrusion was intensified as the background salinity increased and the river discharge decreased. The TGD increased river discharge in winter and weakened the saltwater intrusion. The operation of the TGD is favorable for reducing the burden of freshwater supplement in the highly populated estuarine region. The WDP deceased river discharge, enhanced the saltwater intrusion, especially around the sand bars at the river mouth where the salinity experienced a notable increase, and was unfavorable for freshwater supply in the estuary.

Author details

Jianrong Zhu*, Hui Wu, Lu Li and Cheng Qiu

*Address all correspondence to: jrzhu@sklec.ecnu.edu.cn

State Key Laboratory of Estuarine and Coastal Research, East China Normal University, Shanghai, China

References

[1] Lyu H, Zhu J. Impact of the bottom drag coefficient on saltwater intrusion in the extremely shallow estuary. Journal of Hydrology. 2018;**557**:838-850

[2] Wu H, Zhu J, Chen B, Chen Y. Quantitative relationship of runoff and tide to saltwater spilling over from the north branch in the Changjiang estuary: A numerical study. Estuarine, Coastal and Shelf Science. 2006;**69**(1):125-132

[3] Xiang Y, Zhu J, Wu H. The impact of the shelf circulations on the saltwater intrusion in the Changjiang estuary in winter. Progress in Natural Science. 2009;**19**(2):192-202. (in Chinese)

[4] Li L, Zhu J, Wu H. Impacts of wind stress on saltwater intrusion in the Yangtze estuary. Science China Earth Sciences. 2012;**55**(7):1178-1192

[5] Shen HT, Mao ZC, Zhu J. Saltwater Intrusion in the Changjiang Estuary. Beijing: China Ocean Press; 2003. (in Chinese)

[6] Li L, Zhu J, Wu H, Wang B. A numerical study on water diversion ratio of the Changjiang (Yangtze) estuary in dry season. Chinese Journal of Oceanology and Limnology. 2010; **28**(3):700-712

[7] Zhu J, Wu H, Li L, Wang B. Saltwater intrusion in the Changjiang estuary in the extremely drought hydrological year 2006. Journal of East China Normal University (Natural Science). 2010;**4**(1):1-6. (in Chinese)

[8] Qiu C, Zhu J, Gu Y. Impact of seasonal tide variation on saltwater intrusion in the Changjiang River estuary. Chinese Journal of Oceanology and Limnology. 2012;**30**(2): 342-351

[9] Li L, Zhu J, Wu H, Guo Z. Lateral saltwater intrusion in the north channel of the Changjiang estuary. Estuaries and Coasts. 2014;**37**(1):36-55

[10] Zhu J, Ding P, Zhang L, Wu H, Cao H. Influence of the deep waterway project on the Changjiang estuary. In: The Environment in Asia Pacific Harbours. Netherlands: Springer; 2006. pp. 79-92

[11] Xu K, Zhu J, Gu Y. Impact of the eastern water diversion from the south to the north project on the saltwater intrusion in the Changjiang estuary in China. Acta Oceanologica Sinica. 2012;**31**(3):47-58

[12] Qiu C, Zhu J-R. Influence of seasonal runoff regulation by the three gorges reservoir on saltwater intrusion in the Changjiang River estuary. Continental Shelf Research. 2013; **71**(6):16-26

[13] Qiu C, Zhu J. Assessing the influence of sea level rise on salt transport processes and estuarine circulation in the Changjiang River estuary. Journal of Coastal Research. 2015;**31**: 661-670

[14] Zhu J, Bao D. The effects of river regime changes in the Changjiang estuary on hydrodynamics and salinity intrusion in the past 60 years I. River regime changes. Acta Oceanologica Sinica. 2016;**38**(12):11-22. (in Chinese)

[15] Pritchard DW. The dynamic structure of a coastal plain estuary. Journal of Marine Research. 1956;**15**(1):33-42

[16] Simpson JH, Brown J, Matthews J, Allen G. Tidal straining, density currents, and stirring in the control of estuarine stratification. Estuaries. 1990;**13**(2):125-132

[17] Geyer WR. The importance of suppression of turbulence by stratification on the estuarine turbidity maximum. Estuaries. 1993;**16**(1):113-125

[18] Blumberg AF, Mellor GL. A description of a three-dimensional coastal ocean circulation model. In: Three-Dimens Coast Ocean Models. 1987. pp. 1-16

[19] Blumberg AF. A primer for ECOM-si. In: Tech Rep HydroQual. 1994. p. 66

[20] Chen C, Zhu J, Ralph E, Green SA, Budd JW, Zhang FY. Prognostic modeling studies of the Keweenaw current in Lake Superior. Part I: Formation and evolution. Journal of Physical Oceanography. 2001;**31**(2):379-395

[21] Mellor GL, Yamada T. A hierarchy of turbulence closure models for planetary boundary layers. Journal of the Atmospheric Sciences. 1974;**31**(7):1791-1806

[22] Mellor GL, Yamada T. Development of a turbulence closure model for geophysical fluid problems. Reviews of Geophysics. 1982;**20**(4):851-875

[23] Galperin B, Kantha LH, Hassid S, Rosati A. A quasi-equilibrium turbulent energy model for geophysical flows. Journal of the Atmospheric Sciences. 1988;**45**(1):55-62

[24] Wu H, Zhu J. Advection scheme with 3rd high-order spatial interpolation at the middle temporal level and its application to saltwater intrusion in the Changjiang estuary. Ocean Model. 2010;**33**(1):33-51

[25] Zhu J, Wu H, Li L. Hydrodynamics of the Changjiang estuary and adjacent seas. In: Ecological Continuum from the Changjiang (Yangtze River) Watersheds to the East China Sea Continental Margin. Cham: Springer; 2015. pp. 19-45. (Estuaries of the World)

[26] Smagorinsky J. General circulation experiments with the primitive equations. Monthly Weather Review. 1963;**91**(3):99-164

[27] Large WG, Pond S. Open ocean momentum flux measurements in moderate to strong winds. Journal of Physical Oceanography. 1981;**11**(3):324-336

[28] Editorial Board for Marine Atlas. Ocean Atlas in Huanghai Sea and East China Sea (Hydrology). Beijing: China Ocean Press; 1992

[29] Wu H, Zhu J. Analysis of the transport mechanism of the saltwater spilling over from the north branch in the Changjiang estuary in China. Acta Oceanologica Sinica. 2007;**29**(1): 17-25. (in Chinese)

IntechOpen